Laser-induced level shifts and splittings in multiphoton pair creation

D. D. Su, Y. T. Li, Q. Su, and R. Grobe

Phys. Rev. D **103**, 074513 — Published 30 April 2021
DOI: 10.1103/PhysRevD.103.074513

Laser-induced level shifts and splittings in multiphoton pair creation

D.D. Su[1,2], Y.T. Li[1,2,3], Q. Su[4] and R. Grobe[4]

(1) Beijing National Laboratory for Condensed Matter Physics, Institute of Physics,
Chinese Academy of Sciences, 100190 Beijing, China

(2) School of Physical Sciences, University of Chinese Academy of Sciences,
100049 Beijing, China

(3) Songshan Lake Materials Laboratory, 523808 Dongguan, Guangdong, China

(4) Intense Laser Physics Theory Unit and Department of Physics
Illinois State University, Normal, IL 61790-4560, USA

Using numerical solutions to the Dirac equation, we examine the role of energy shifts on the energy spectrum of created positrons in the laser-induced electron-positron pair creation process in the presence of a highly charged model nucleus. We suggest that at those laser intensities, where the created electrons can be captured by the nucleus, the inclusion of the field induced energy level shifts is crucial to predict correct positron energy spectra, especially close to the threshold for this process with regard to the laser frequency. For the interesting case where the laser frequency is tuned to the bound state energy differences, the coherence associated with possible electronic Rabi oscillations is transferred to the generated positrons leading to new splitted peaks in their energy spectrum.

1. Introduction

The possibility to break down the vacuum state and to create electron-positron pairs from either a supercritical time-independent or electromagnetic fields has been a subject of wide interest [1, 2]. In part, this interest to probe the nonlinear properties of the quantum vacuum has also been fostered by dramatic advances in the development of lasers with unprecedented strength [3-7]. Here intensities of the order of $10^{24} \sim 10^{26}$W/cm^2 may become accessible in the next few years, which might open the door to exciting investigations of QED in the high-intensity regime. A firm theoretical understanding of relativistic effects is important not only for studying fundamental aspects of high-intensity laser-matter interaction, but also for applications such as novel X- and gamma-ray radiation sources.

A monochromatic plane wave field can model the electromagnetic field of a laser beam where all of the photons have the same energy and propagate in the same direction. This configuration cannot trigger any pair creation process from the vacuum, which usually requires the collision of two or more photons. However, by choosing external field configurations that are more complicated with regard to their spatial and temporal characteristics, photon-photon collisions can be simulated leading to the pair production process [8-11]. An alternative way to create electron-positron pairs is based on a static but supercritical electric field associated with a highly charged nucleus. Yet another configuration to produce pairs relies on the simultaneous action of a nuclear binding field and an electromagnetic field. Here the bound states [12-17] of the binding potential can serve as a bridge between the positive and negative energy continuum states and therefore enhance the pair production. This scenario can be realized in the laboratory by injecting a laser pulse at a highly charged ion or nucleus. The energies of the bound states play a major role in the pair creation processes induced by continuum-bound state interactions [13-15,18,19].

In this work, the focus is on two new aspects of the pair creation process and the resulting energy spectra of the created positrons that have not received attention. Both illustrate how spectral features of the final electron states manifest themselves in the energy distribution of the created positrons. First, it is pointed out that in addition to the well-understood threshold shifts associated with the negative energy continuum states, the inclusion of the dressing of the corresponding electronic bound state energies is also crucially important at these high laser intensities. These shifts need to be understood in order to correctly identify the positrons' energy peaks with the corresponding multiphoton transitions.

Second, for the interesting case where the laser frequency is tuned close to the resonance of a pair of electronic bound states, a new phenomenon is predicted. We report on a novel two-photon based coherence transfer phenomena, where resonant bound-bound transitions of the captured electron can manifest itself in the splitting of peaks in the positrons' energy spectra triggered by a single laser pulse of fixed frequency.

A different effect based on resonant Rabi-oscillations in the context of pair creation was discussed in a seminal work by Ruf et al. [20]. In this interaction there was no binding potential and the field was given by two counter-propagating beams. A splitting was observed in the final particle yield as a function of the laser frequency associated with the fact that the vacuum was modeled by a single Gaussian wave packet of negative energy centered around zero momentum. As a result, the Rabi oscillations occurred between relevant continuum states of negative and positive energies.

The paper is structured as follows. In Section 2 we introduce the model system focusing on the relevant energy scales of the pair creation dynamics. In Section 3 we propose to calculate the laser-induced energy shifts via a time-averaging approach. In Section 4 the drastic impact of the bound state level shifts on the pair creation behavior close to the threshold is demonstrated. In Section 5 we show how each of the spectral features of the positrons can be associated with a unique multi-photon process involving the electron capture into a dressed bound state. In Section 6 we report on the new coherence transfer phenomenon. We complete this work with an outlook on future challenges.

2. The model system and its bare energies

In this work, we model the interaction of the quantum vacuum state with the external laser field and the static electric field associated with a highly charged nucleus by the time-dependent Dirac equation [21] for the electron-positron field operator $\Psi(\mathbf{r},t)$. It is given by

$$i \hbar\, d\Psi/dt = c\, \boldsymbol{\alpha}\, [\mathbf{p} - q\, \mathbf{A}(\mathbf{r},t)/c]\, \Psi + m\, c^2\, \beta\, \Psi + qV(\mathbf{r})\, \Psi \qquad (2.1)$$

where $\boldsymbol{\alpha} \equiv (\alpha_1, \alpha_2, \alpha_3)$ and β are the usual set of the four 4×4 Dirac matrices, $\mathbf{A}$ and V are the vector and scalar potentials describing the two external fields, m is the electron's mass and q is its charge. Here the external laser field is described by a linearly polarized monochromatic electro-magnetic field that travels along the x-direction and whose electric (magnetic) field component points along the y- (z-) direction, given by the vector potential $\mathbf{A}(x,t) = A_0 \, \mathrm{Cos}(\omega t - kx) \, \mathbf{e}_y$. For simplicity, we model the binding force of the nucleus centered at $\mathbf{r}=0$ by a short-range potential well V(x) of strength V_0. While their chosen space-time dependences can be considered as a perturbative form of more realistic space-time configurations, their impact of the dynamics is treated "exactly", meaning the numerical error in all simulations can be well controlled by varying the space-time grid parameters.

We have chosen to examine this particular field configuration in order to focus solely on relativistic effects triggered by the combination of the laser's electric and magnetic field components. In the absence of the magnetic field component of the laser and for small particle velocities (compared to the speed of light c), the resulting dynamics along the x- and y- direction is decoupled, as the binding force $-qV'(x) \, \mathbf{e}_x$ is chosen perpendicular to the oscillatory electric field component of the laser $A_0 \, \omega/c \, \mathrm{Sin}(\omega t) \, \mathbf{e}_y$.

In our first Figure we have sketched the relevant energy scales of the pair creation dynamics.

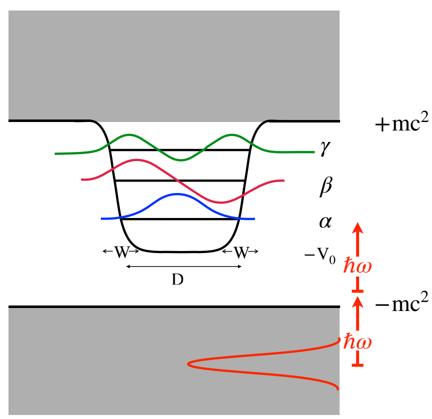

Figure 1 Sketch of the relevant bare energy scales, the shape of the binding potential and the three bound states, which can become populated during the pair creation process.

In the absence of any mutual interaction, there are five energy scales (mc^2, E_α, E_β, E_γ and $\hbar\omega$) that are relevant for our dynamics. The first and most obvious scale mc^2 characterizes the bare vacuum, which -due to its central importance- is being used from now on as the unit scale for all energies. Second, the lowest three bound state energies of the binding potential, denoted by E_α, E_β and E_γ ($E_\alpha<E_\beta<E_\gamma$) depend solely on three parameters, given by the potential's spatial width D, its spatial turn-on and -off length w, and its depth V_0. This potential is given here as V(x) =

$V_0\{-S[(x+D/2)/w] + S[(x-D/2)/w]\}$, based on two shifted smooth potential steps given by the famous Sauter Tanh-potential $S(x) \equiv [1+\text{Tanh}(x)]/2$, which has been often used in theoretical pair creation studies [19, 22-25]. It is attractive for the electron and correspondingly repulsive for the positron. Due to its short-ranged nature it can support only a finite number of bound states into which the created electrons can be captured [19,24,25]. Due to the absence of sharp corners, the spatially smoothed potential is numerically easier to handle for finite space-time grid methods than a simple box.

The energies of these bound states can be determined numerically from the eigenvalue problem $H_0 |E\rangle = E |E\rangle$, where $H_0 \equiv c\, \alpha_x\, p_x + m\, c^2\, \beta + qV(x)$ denotes the time-independent part of the Dirac Hamiltonian in the absence of the laser field. We have assumed the two fermionic momenta along the y- and z-direction to vanish. For a spatially narrow potential with $D = 3.428\ \lambda$ [where $\lambda \equiv \hbar/(mc)$ denotes the reduced Compton wavelength of the electron], $w = 0.3\ \lambda$ and $V_0 = 1.8\ mc^2$, it supports three bound states with bare energies found at $E_\alpha/(mc^2) = -0.5$, $E_\beta/(mc^2) = 0.07$ and $E_\gamma/(mc^2) = 0.65$. The fifth energy scale, $\hbar\omega$, is associated with the energy of the laser's photon, which we have varied in our numerical simulations between $\hbar\omega/(mc^2) = 0.4$ and 0.8.

In most calculations of computational quantum field theory, the initial vacuum state is modelled by the set of negative energy eigenstates of the force-free Dirac Hamiltonian with energies $-(m^2c^4+c^2p^2)^{1/2}$. Each state is then evolved in time and then the corresponding transition matrix elements between these states and positive and negative energy eigenstates are used to determine observable quantities such as the positrons' energy spectra or the vacuum decay probabilities [24,26]. In order to avoid any turn-on effects due to the laser field and to simulate a truly adiabatic scenario, we have replaced the usual negative energy states with the Volkov states [27-32], i.e., with time-dependent solutions to the Dirac Hamiltonian of Eq. (2.1) but with $V(x) = 0$. As these Volkov solutions are analytically available, the laser's effect on the continuum states (in the absence of the binding force) is therefore treated exactly. In order to minimize the effects due to a sudden turn on of the potential, during the first cycle of the interaction ($0<t<2\pi/\omega$) we have multiplied $V(x)$ with the smooth amplitude $\sin^2[\omega t/(2\pi)]$. As we incorporate the dressing effects of the laser onto the negative energy continuum via the Volkov states, the onset of the vaccum's decay is characterized by the turn-on of the binding force.

3. Field induced corrections to the continuum and discrete bare energies

While the energy scales discussed above characterize some aspects of the vacuum decay process, due to the large required laser intensities for pair creation, the induced level shifts associated with the full laser-nucleus-vacuum interaction can be quite important even qualitatively. This is especially true when the lowest bare energy is close to the threshold condition for pair-creation, i.e. $-mc^2 + 2\hbar\omega = E_\alpha$, where the highest lying negative energy continuum states $|\mathbf{p}=0\rangle$ can just barely couple to the potential's ground state under the absorption of two photons.

In the absence of the nucleus, the main effect of the field is an effective dressing on the vacuum states with negative energies $E_p = -[m^2 c^4 + c^2p^2]^{1/2}$, leading to an energy shift with regard to the first bare energy scale mc^2. This correction can be modelled by an effective relativistically increased mass m^*. As this effect has been discussed already in the literature [33-37] in sufficient detail, we just state the final expression $E_p(\xi) = [m^*(\xi)^2 c^4 + c^2p^2]^{1/2}$, where the relativistic mass m^* is given as $m^*(\xi) = m(1 + \xi^2/2)^{1/2}$. We note that this energy shift is not a function of A_0 and ω independently but depends solely on the unitless parameter $\xi \equiv |qA_0/(mc^2)|$. This normalized amplitude of the vector potential plays a similar role for pair creation as the (inverse of the) Keldysh parameter [38] does for atomic photoionization in strong fields [39-42]. This scale is also related to the average (ponderomotive) energy of a free electron or positron in the laser field.

As the ground state energy E_α of the binding field was chosen to be above the negative energy continuum threshold $-mc^2$, the potential is subcritical and therefore cannot induce any electron-positron pair creation by itself. In the absence of any laser field, a supercritical nucleus could only create pairs by itself if $E_\alpha < -mc^2$, i.e., when the bound state has dived into the negative energy continuum [43].

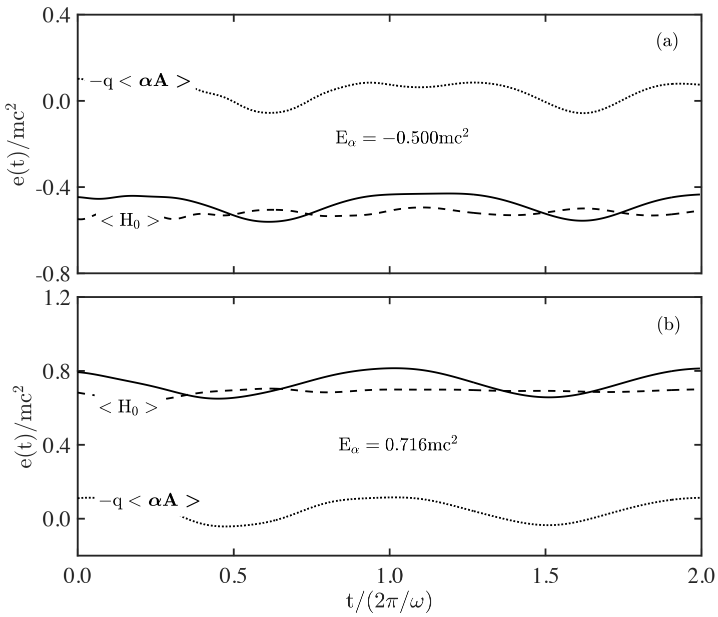

Figure 2 (a) The time-dependence of the energy $e(t) \equiv \langle\alpha(t)|\, H(r,t)\, |\alpha(t)\rangle$ for an electron that is initially in the ground state $|\alpha\rangle$ for the potential used in our calculations (with $V_0 = 1.8\ mc^2$, $w = 0.3\ \lambda$, $D = 3.428\ \lambda$, $\hbar\omega = 0.48\ mc^2$ and $\xi = 0.5$).
(b) For comparison, we also show e(t) for a much weaker bound and non-relativistic ground state with energy $E_\alpha = 0.716\ mc^2$, obtained for a different binding potential with $V_0 = 0.47\ mc^2$, $w = 0.1\ \lambda$, $D = 3\ \lambda$, $\hbar\omega = 1.0\ mc^2$ and $\xi = 0.5$). The dashed and dotted lines are the contributions to e(t) from $\langle H_0\rangle$ and $-q\ \langle \boldsymbol{\alpha}\ \mathbf{A}\rangle$, respectively.

Due to the interaction with the laser field, the effective energy of the bound states [44,45] can be shifted. In order to estimate these shifts in a non-perturbative manner, we propose here to determine their dressed energies by computing the time-dependent energy first, defined by the expectation value $e(t) \equiv \langle\phi(t)|\, H\, |\phi(t)\rangle$. Here the quantum mechanical state $|\phi(t)\rangle$ is the time evolved bound state under the Dirac equation with the initial condition $|\phi(t{=}0)\rangle = |E\rangle$, where $|E\rangle$ is one of the three bound states $|\alpha\rangle$, $|\beta\rangle$ or $|\gamma\rangle$, which satisfy $H_0\, |E\rangle = E\, |E\rangle$. While the main quantum field theoretical simulations of the vacuum decay have the three bound states initially unoccupied, we use here simple quantum mechanical calculations, where the bound state is fully populated. In the absence of the laser field ($A_0{=}0$), this expectation value e(t) is naturally constant $\langle\phi(t)|\, |H_0\, |\phi(t)\rangle = E$, reproducing the bare state energy. The time dependence of e(t) is the result of the contributions due to the non-trivial evolution of the state $|\phi(t)\rangle$ involving transitions to other states as well as due to the laser's periodic behavior $e(t) = \langle\phi(t)|\, H_0\, |\phi(t)\rangle - q\ \langle\phi(t)|\ \boldsymbol{\alpha}\ \mathbf{A}(x,t)\ |\phi(t)\rangle$.

In Figure 2 we have graphed this time dependence for the ground state $|\alpha\rangle$. We find that e(t) is almost periodic with the laser's period $T = 2\pi/\omega$, which suggests that irreversible transitions can be neglected. However, the variations of e(t) with regard to E_α do not average out to zero. In fact, we propose here that we can potentially use this non-vanishing time-averaged value, defined as $E_\alpha(\xi,\omega) \equiv (1/T) \int_0^T dt\, e_\alpha(t)$, to estimate the dressed energy level shift for each bound state. This proposal is, of course, similar to the derivation above leading to the effective mass shift for the Volkov states [27-32].

In order to emphasize that the particular time-dependence of e(t) for our relativistic bound state $|\alpha\rangle$ is not necessarily generic, we have included in Figure 2b the corresponding energy for a more weakly bound ground state as well. This time-dependence is qualitatively different as the energy follows here almost directly the sinusoidal time-dependence of the laser's electric field. However, in both cases, the overall energy shift (0.0157 mc^2 for Fig. 2a and 0.0120 mc^2 for Fig. 2b) is caused by a relatively larger upward shift of the average of $-q \langle\phi(t)|\, \boldsymbol{\alpha}\, \mathbf{A}(x,t)\, |\phi(t)\rangle$ (0.0395 mc^2 and 0.0484 mc^2, respectively) than the observed down shifts due to $\langle\phi(t)|\, H_0\, |\phi(t)\rangle$.

In Figure 3 we have graphed the calculated effective energies $E_\alpha(\xi,\omega)$, $E_\beta(\xi,\omega)$ and $E_\gamma(\xi,\omega)$ of the three bound states as a function of the scaled laser's amplitude ξ for two frequencies ω.

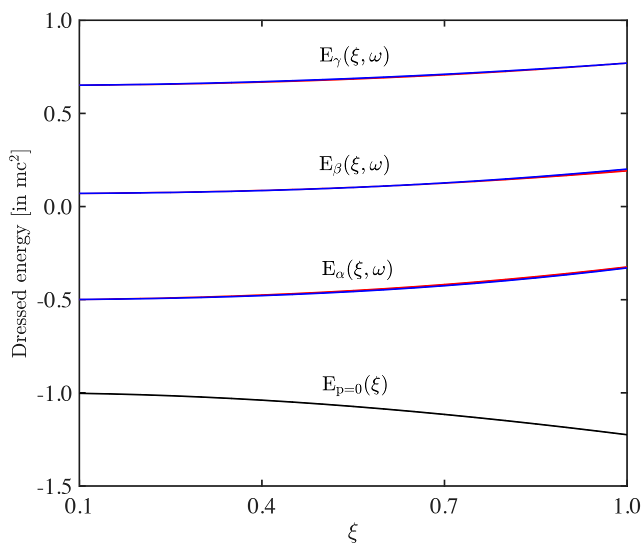

Figure 3 The three dressed bound state energies $E(\xi,\omega)$ as a function of the scaled field strength ξ for the laser frequencies $\hbar\omega/(mc^2) = 0.45$ and 0.55. For comparison, we have also included the threshold shift $E_{p=0}(\xi) = -m\,(1 + \xi^2/2)^{1/2}\, c^2$.

We see that the dressing increases the effective energies in a monotonic fashion. For example, for ξ=1, the ground state energy is shifted up from $E_\alpha = -0.5\ mc^2$ to $-0.33\ mc^2$, corresponding to a significant 34% increase. This emphasizes the importance of these energy shifts in the pair creation regime. For comparison, we have also included the energy of the highest lying negative energy continuum state, whose energy is shifted down from $E_{p=0} = -m\ c^2$ to $E_{p=0}(\xi) = -m\ (1 + \xi^2/2)^{1/2}\ c^2$. While the dressing of the vacuum state is strictly only a function of the ξ, the bound state energies depend also on ω separately. However, for the frequency range considered in our work, the data in Figure 3 suggest only a weak frequency dependence.

We should point out that while these novel calculations of the dressed energy levels are in principle non-perturbative and therefore differ from traditional derivations of AC Stark-shifts as common in atomic ionization physics [46,47]. However, our approach has also its limitations with regard to the laser intensity. The temporal energy average was performed during the first cycle of the constant amplitude region after its turn on. If the laser intensity is sufficiently large that already a significant amount of population can be irreversibly transferred to other states, the resulting time-dependent energy is no longer periodic and the value of this period-average would crucially depend on during which cycle the average was performed.

4. Threshold shifts due the laser dressing

Including the laser dressing of the vacuum state as well as the bound states, one could conjecture that the minimal frequency required for the occurrence of the pair creation would generalize from $-mc^2 + 2\ \hbar\omega = E_\alpha$ to the dressed form $-m^*(\xi)\ c^2 + 2\ \hbar\omega = E_\alpha(\xi,\omega)$. As the external field shifts the ground state energy upward and the upper edge of the negative energy continuum is shifted downward, the smallest required photon energy might therefore be increased from $\hbar\omega = (E_\alpha + mc^2)/2$ to the larger threshold value

$$\hbar\omega\ =\ [E_\alpha(\xi,\omega) + m^*(\xi)\ c^2]/2 \tag{4.1}$$

To test this conjecture, in Figure 4 we have computed the total positron yield after the interaction with the laser field with $\xi = 0.5$ for a continuous range of photon energies. The left most graph corresponds to a system where the potential's parameters were chosen to support a ground state at energy $E_\alpha = -0.6\ mc^2$. According to the threshold condition based solely on the bare state energies, we would expect the pair-creation to set in at a minimal photon energy of $\hbar\omega = 0.2\ mc^2$ as indicated by the arrow. However, the observed energy of $\hbar\omega = 0.26\ mc^2$ is larger by 30% , as the result of the two shifts. Here the bare state shifted up by 9.8% (from $-0.6\ mc^2$ to $-0.541\ mc^2$) and the relevant continuum state shifted down by 6.1% (from $-mc^2$ to $-1.061\ mc^2$). Therefore, small percentage changes in the level energy can lead to drastic relative changes in the required photon energy. This observed threshold energies matches the predicted one from Eq. (4.1) very well, as indicated by the vertical reference line. The slight offset to lower photon energies is an interesting but well-known finite-time effect related to the fact that the inverse of the vacuum decay rate effectively widens the effective frequency spectrum of the external laser field. This is the same mechanism that is responsible for the nonzero width of the positrons' energy peak discussed in Section 5 below. It is similar to the power broadening of the electron energy peak in standard photo-ionization [48]. The final positron yield grows with increasing interaction time.

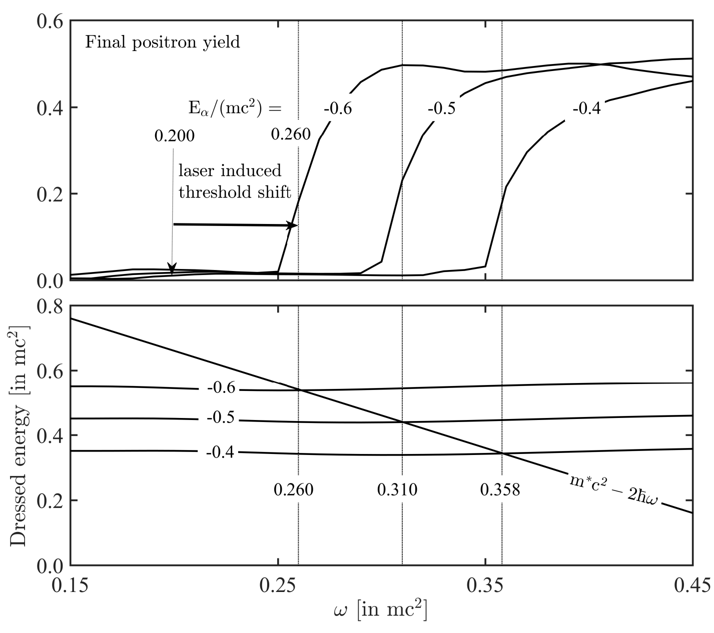

Figure 4 (a) The final number of created positrons after the interaction with the laser field as a function of the laser's photon energy $\hbar\omega$. The arrow indicates the minimal energy according to the threshold condition based on the bare energies. The vertical line is the predicted threshold based on the fully dressed bound state and continuum state energies. The left most curve corresponds to a

nuclear potential with the bare ground state energy $E_\alpha = -0.6\ mc^2$, obtained for $V_0 = 1.85\ mc^2$, D=3.885 λ, w=0.3 λ. The other two curves are for potentials V(x) with higher bare ground state energies $E_\alpha = -0.5\ mc^2$, obtained for $V_0 = 1.8\ mc^2$, D=3.428 λ, w=0.3 λ and with $E_\alpha = -0.4\ mc^2$, obtained for $V_0 = 1.726\ mc^2$, D=3.2 λ and w=0.3 λ. The laser amplitude was ξ=0.5 and the total interaction time T = 900 λ/c.
(b) The dressed energy of the three ground states $E_\alpha(A_0,\omega)$ as a function of the photon energy $\hbar\omega$. The straight line is the prediction of the threshold energy according to Eq. (4.1), i.e., $m^*(\xi)\ c^2 - 2\hbar\omega$, such that the crossing with the curve $E_\alpha(A_0,\omega)$ corresponds to the minimal photon energy for the 2-photon based pair creation process to occur.

While the final positron yield increases rapidly after the threshold frequency has been exceeded, its growth reaches its maximum at around $\hbar\omega \approx 0.3\ mc^2$, after which the final yield begins to decrease. This is related to the fact that the coupling strength to the ground state decreases with increasing amount of the (negative) continuum energy. However, the decrease is not related to the frequency dependence of the dressed ground state energy $E_\alpha(\xi,\omega)$ as we display in Figure 4b. In this Figure we have graphed this dependence, which apparently depends only weakly on ω. Its crossings with the straight line, given by $m^*(\xi)\ c^2 - 2\hbar\omega$, obviously indicates the minimum photon energy required for the two-photon pair creation process to occur. For photon energies larger than $\hbar\omega \approx 0.3\ mc^2$, the decrease of the yield is not strictly monotonic and evolves first into a plateau region. A similar finding was already reported in [49], however, for the case of a spatially independent laser field. In that case it was associated with the interference of several competing decay mechanisms.

To support the universality of the threshold shifts, we have repeated the same simulation for two different (and more weakly) binding potentials by adjusting their shape, for which the bare ground state energies are $E_\alpha = -0.5\ mc^2$ and $E_\alpha = -0.4\ mc^2$. We find that for all three scenarios the pair-production sets in at significantly larger photon energies than suggested by their bare energies. The actual onset is sufficiently accurately determined by the combined energy shifts of the continuum threshold and the ground state.

In addition to the shift for the threshold due to the laser's intensity and frequency, the presence of the laser dressing effects on the continuum and bound states should manifest itself also in the energy spectrum of the created positrons. We will examine this in the next section.

5. Energy spectra of the created positrons

In this section we will calculate energy distributions of the created positrons and interpret their features in terms of multi-photon transitions of even-order between the dressed energies discussed in Sections 3 and 4.

The final state of the created positrons can be described by its distributions with respect to the final velocities, momenta or energies before or after they have left the laser field. These six probability densities can be structurally quite different for electromagnetic fields that are so strong that they can trigger pair creation. In our analysis below, we have focused on the (total) energy spectra of the positrons inside the laser field as they provide in our opinion the best access towards a physical interpretation of the various underlying mechanisms [18]. In contrast to the momentum spectra where the distribution reflects the continuum shifts [20], the positrons' distribution of the final energy is not affected by these particular shifts. This can simplify our theoretical analysis of the complicated spectra. Furthermore, similar processes that differ only by the number of absorbed photons are separated equidistantly on an energy scale.

Traditionally, the initially fully occupied negative energy continuum states are coupled to the two external fields via the negative charge of the electron and the resulting vacancies are therefore associated with the created positrons. Equivalently, using charge conjugation symmetry, one can couple both fields into the dynamics using the positive charge, here our static potential is repulsive (for the positrons). The resulting energy spectrum of the created positrons $\rho_{e+}(E)$ can be computed by projecting each of the time-evolved negative energy Volkov states $|N(t)\rangle$ onto the manifold of Volkov states $|P(E)\rangle$ with the dressed positive energy E, where $E \equiv [m^{*2}c^4+c^2P^2]^{1/2}$. The distribution is given by $\rho_{e+}(E) = \Sigma_N |\langle P(E)|N(t)\rangle|^2$, where the summation extends over all initial states. To be consistent, the total number of created positrons is given by the double summation $\Sigma_N \Sigma_P |\langle P(E)|N(t)\rangle|^2$.

As the energy spectra are better suited for a theoretical analysis, we will use them from now on. In Figure 5 we present the energy distribution of the created positrons for a laser field with photon energy $\hbar\omega/(mc^2) = 0.45$ and scaled laser amplitudes $\xi = 0.5$ and $\xi = 1$. We find that the spectra are rather complicated. But we will argue below that each feature can actually be explained in terms of multiphoton transitions between the corresponding dressed continuum and discrete states. Here the energy shifts due to the dressing discussed above are essential for these interpretations.

The enhancement of pair creation manifest by the occurrence of the peaks is caused by the availability of the discrete energies of the final electronic bound states [49,50] as well as an enhanced coupling between the threshold states for positive and negative energy. To better guide the eye, we have denoted with dashed vertical lines the corresponding predicted positron energies. There are two types of transitions. The first ones are characterized by processes where the final electron can be captured in the dressed bound states. For example, we denote with α_n those predicted positron energies, where the pair-creation process (involving the absorption of n photons) is characterized by the capture of the associated electron in the dressed ground state $|\alpha\rangle$. The peak energies are predicted to occur at $\alpha_n = |E_\alpha(\xi) - n\,\hbar\omega\,|$.

In Figure 5a we see that the actual energy (≈ 1.35 mc^2) of the observed dominant peak α_2 matches perfectly with the prediction $|E_\alpha(\xi) - 2\,\hbar\omega\,| = |-0.46 - 2\times 0.45\,|$ mc^2. In fact, any mismatch would be less than the numerical accuracy of our calculations. Due to the rather long interaction time (which amounts to 50 laser periods), the peak widths are rather narrow. The quasi-oscillatory substructures around each peak are likely associated with the fact that the interaction with the binding force was relatively abruptly turned on (over one laser cycle). The additional peaks, labelled α_4 and α_6, are shifted by precisely 2 $\hbar\omega$ and 4 $\hbar\omega$ from α_2 and therefore correspond to four- and six-photon processes with an electron capture into the same dressed ground state $|\alpha\rangle$. We also see clearly the dynamical relevance of the first and second excited states $|\beta\rangle$ and $|\gamma\rangle$, which can be reached only under the absorption of at least four and six photons. The observed energies of each of these four peaks agree again perfectly with the predictions (four lines denoted by β_4, β_6, γ_4 and γ_6) based on the dressed energies obtained from the period averaged energy expectation values derived in Section 3 above. We have used $E_\beta(\xi) = 0.097$ mc^2 and $E_\gamma(\xi) = 0.6783$ mc^2 as can be read off the data shown in Figure 3 above.

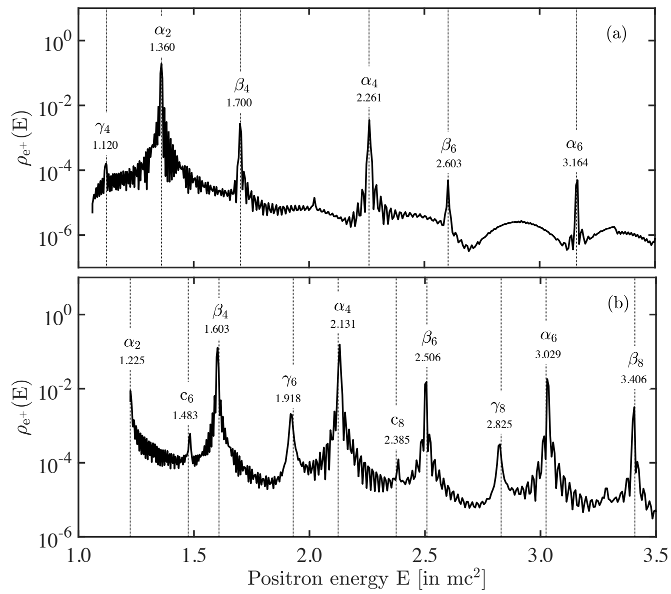

Figure 5 Final energy spectra $\rho_{e+}(E)$ of the created positrons after the interaction of the vacuum state with a laser field of frequency $\omega = 0.45\ mc^2/\hbar$ and scaled field strength $\xi = 0.5$ (a) and $\xi = 1$ (b). As a reference, the dashed vertical lines are the predicted peak positions based on the assumption that the created electron is trapped in a laser-dressed bound state. The interaction time was 50 laser cycles.

In separate simulations, we found that peak amplitudes (α_4 and β_4) and (α_6 and β_6) associated with the absorption of the same number of photons follow a similar perturbative power law scaling $\sim \xi^{2n}$ with increasing laser intensity, as expected. However, they also have a remarkably similar peak height, which suggests that the coupling strengths of the continuum state to the lowest two bound states are rather comparable.

In Figure 5b we show the positron energy spectra for a larger laser field amplitude $\xi = 1$. Compared to the peak locations for the lower intensity $\xi = 0.5$, we find here even more significant energy red shifts as well as substantial changes in their peak strengths. For example, α_2, which was the dominant peak for all amplitudes $\xi < 0.8$, has now shifted to the energy threshold at 1.22 mc^2, showing that (due to a significant energy dressing) the pair creation with electron capture in the ground state requires now at least 4 photons. We also see that in the same energy range as shown in Figure 5a, there are now also the 8-photon peaks β_8 and γ_8 visible. This perfect match gives again credence to the validity of method we used to calculate the dressed energies in section 3. Here we have used $E_\alpha(\xi) = -0.3241\ mc^2$, $E_\beta(\xi) = 0.1917\ mc^2$ and $E_\gamma(\xi) = 0.7704\ mc^2$, as can be read off the data shown in Figure 3 above.

Overall, the spectrum looks rather different from the spectrum for $\xi = 0.5$. In fact, we even observe the occurrence of new peaks at positron energies 1.48 mc^2 and 2.38 mc^2, which we have labelled as c_6 and c_8. The physical origin of these 6- and 8-photon peaks is not associated with the final capture of the electrons in any bound state. The energy locations of these two new peaks are slightly above the energy difference between the edges of the downward shifted lower energy ($-m^*c^2$) and the upward shifted upper energy (m^*c^2) continuum states. In other words, we have $c_n = - m^*c^2 + n \hbar\omega = (-1.061 + n\, 0.45)\, mc^2$ with n=6 and n=8.

We have to point out that these interesting peaks c_6 and c_8 do *not* reflect the beginning of the solely laser-induced pair creation process, which has been studied widely in the literature. We remind the reader here that these traditionally studied laser induced continuum-continuum transitions would require the collision of at least two photons, which are not possible for our chosen electromagnetic field configuration provided by a plane wave configuration with only a single propagation direction. The generation of those electron-positron pairs could be modeled for example by two counter-propagating electromagnetic waves. The occurrence of the two peaks c_6 and c_8, however, is therefore an interesting consequence of the interaction with the binding potential. In fact, the absence of these two peaks for a repeated simulation performed for $V_0 = 0$ confirms this idea.

6. Autler-Townes split positron energies

For the entire frequency regime $0.45 < \hbar\omega/(mc^2) < 0.65$ that we studied, all spectral feature can be explained based on multi-photon transitions between dressed energy levels. For the region where the energy of two photons roughly matches the bare energy difference between two bound states, we observe an interesting novel mechanism that can further complicate the positron spectra. For the parameters of the potential discussed above, the bare energy level differences $E_\gamma - E_\beta = 0.58\, mc^2$ and $E_\beta - E_\alpha = 0.57\, mc^2$ suggest that a laser with photon energy $\hbar\omega = 0.55\, mc^2$ could lead to interesting new resonance phenomena associated with Rabi-like transitions [51] of the captured electrons.

In Figure 6 we present similar positron energy spectra as in Figure 5, but this time for a larger frequency $\omega = 0.55\, mc^2/\hbar$. As expected, for the lower laser intensity ($\xi = 0.5$) the date in Figure 6a recover the peaks α_2, α_4, β_4 and β_6 at their predicted energies. However, the peaks γ_4 and γ_6 seem to have vanished. According to the numerical values of the dressed bound state energies (E_α = -0.4646 mc^2, E_β = 0.0961 mc^2, E_γ = 0.6814 mc^2) for these laser parameters, we would expect that the corresponding peaks associated with the γ_4 and γ_6, processes to be very close to the locations of the α_2 and α_4 peaks. As the corresponding processes require the absorption of two additional photons, the amplitudes of the γ_4 and γ_6 peaks are orders of magnitude less than those of the corresponding α_2 and α_4 as already shown in Figure 5. We also confirmed these amplitude differences in the data obtained for the larger laser frequency ω = 0.65 mc^2/$\hbar$. Therefore, these two peaks cannot be resolved as they compete with the energy of other more dominant peaks.

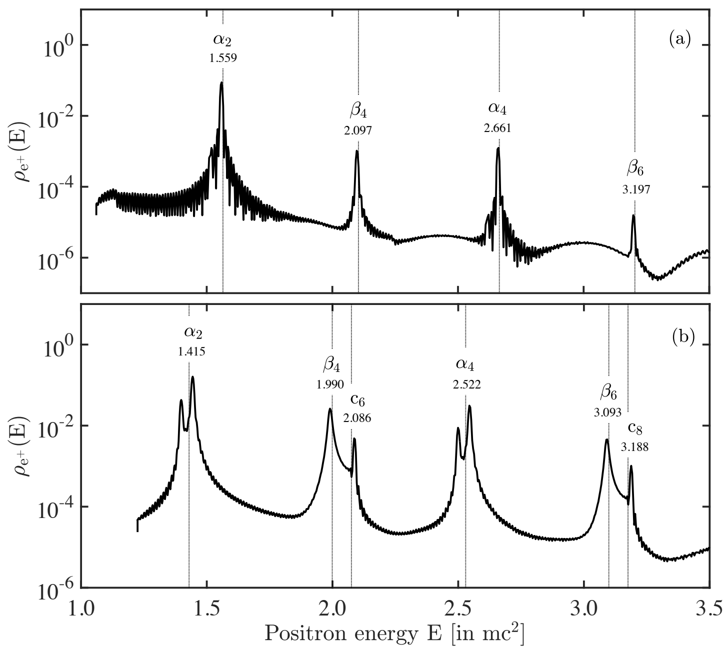

Figure 6 Final energy spectra of the created positrons after the interaction of the vacuum state with a laser field of frequency ω = 0.55 mc^2/$\hbar$ and scaled field strength ξ = 0.5 (a) and ξ = 1 (b). As a reference, the dashed vertical lines are the predicted peak positions based on the assumption that the created electron is trapped in a laser-dressed bound state.

In Figure 6b we have increased the laser intensity (ξ = 1) such that now the amplitude of the two peaks c_6 and c_8 that were based on the interaction of the dressed continuum edges are sufficiently large to be present again. This is very similar to their occurrence as we increased the laser intensity for ω = 0.45 mc^2/$\hbar$ (as shown in Figure 5). The data in Figure 6b for the larger laser intensity (ξ = 1) indicate an interesting novel feature, the peaks α_2 and α_4 appear to be split around those values that were predicted based solely on the level shift analysis in Section 3.

One could first conjecture that this splitting of the positron energy peak is a consequence of the bound-bound resonance between the lowest two bound states $|\alpha\rangle$ and $|\beta\rangle$, as after all their energy spacing happens to be close to the photon energy. From numerous theoretical and also experimental quantum optical studies, it is well known that Rabi-oscillation between two (or more) bound states can be understood in terms of Autler-Townes splitting [52] leading to the well-known Mollow triplet in the fluorescence spectrum [53]. However, to be fully consistent, this particular mechanism would require that also the corresponding β_2 and β_4 levels need to be split. However, neither of the two β peaks are actually split and appear precisely at their predicted positions $|E_\beta(\xi) - n\,\hbar\omega\,| = |0.2011 - n\,0.55|\,mc^2$ for n=2 and n=4, as indicated by the dashed vertical lines.

It turns out that in our electromagnetic field configuration, where the forces of the laser's electric field component and the binding force are perpendicular to each other, the direct single photon coupling between the first excited state $|\beta\rangle$ and its neighbors $|\alpha\rangle$ and $|\gamma\rangle$ is actually rather small, while the quasi-resonant 2-photon coupling between $|\alpha\rangle$ and $|\gamma\rangle$ is more important. This means that the split of the positronic α_2 and α_4 energy peaks are the result of the resonant 2-photon Rabi-like transitions between the *electronic* states $|\alpha\rangle$ and $|\gamma\rangle$. In order to prove the dynamical relevance of the second excited state $|\gamma\rangle$, we have repeated the same simulation for a weaker binding force (V_0 =1.1 mc^2, w = 0.3 λ, D = 3.2 λ) for which this second excited state $|\gamma\rangle$ is absent, but we still satisfy the required resonance condition $E_\beta - E_\alpha \approx \hbar\omega$. The resulting positron spectra shown in Figure 7 show that the α lines are indeed no longer split.

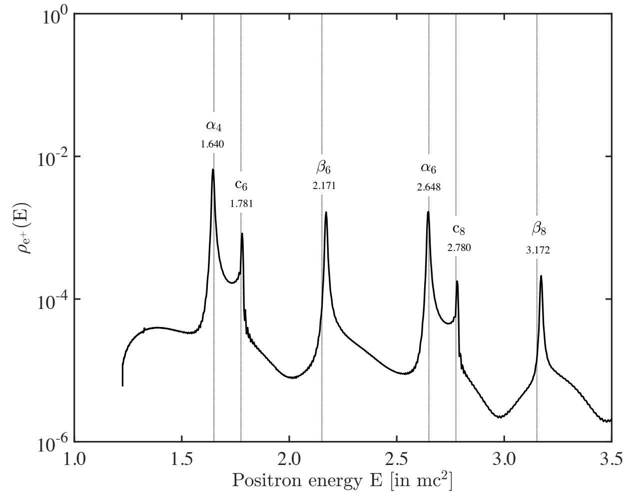

Figure 7 Final energy spectra of the created positrons after an interaction of the vacuum state with a laser field of scaled field strength $\xi = 1$. As a reference, the dashed vertical lines are the predicted peak positions based on the assumption that the created electron is trapped in a laser-dressed bound state. Here the binding potential (V_0 =1.1 mc^2, w = 0.3 λ, D = 3.2 λ) has only two bound states at energies E_α= 0.1648 mc^2 and E_β = 0.6682 mc^2, which are in close resonance for the chosen photon energy $\hbar\omega$ = 0.5 mc^2.

In order to "re-activate" the $|\alpha\rangle$ and $|\beta\rangle$ transition probability, we could modify our external laser field by permitting the simultaneous collision of two photons. In order to model two counter-propagating laser beams one could consider the new vector potential given by $\mathbf{A}(x,t) = A_0/2\ [\mathrm{Sin}(\omega t - k\,x) + \mathrm{Sin}(\omega t + k\,x)]\ \mathbf{e}_y = A_0\ \mathrm{Cos}(k\,x)\ \mathrm{Sin}(\omega t)\ \mathbf{e}_y$, which can be approximated [54,55] close to the node of the resulting standing wave by a purely time-dependent electric field $\mathbf{A}(t) = A_0\ \mathrm{Sin}(\omega t)\ \mathbf{e}_y$. The positron spectrum for this different system reveals that here *both* the α_2 as well as the β_4 lines are Autler-Townes split as expected.

7. Summary and outlook into future challenges

In this work we have studied the electron-positron pair creation process triggered by a laser field configuration where all photons propagate along the same direction. Normally, due to the absence of photon-photon collisions, the traditional vacuum decay process cannot occur. However, the additional presence of a sub-critical binding force triggers the pair production process, in which the created electron can be subsequently captured by the bound states of the binding field. We have shown that an accurate description of the laser dressing of the vacuum, represented by negative energy continuum states as well as dressing of the bound state energies are important to interpret the energy spectra of the created positrons.

For the special case where the laser frequency permits a resonant two-photon transition between two electronic bound states, the resulting positron energy peaks are split, manifesting a novel coherence transfer effect from the electrons to the positrons. While usually the Autler-Townes splitting has been measured with regard to the three-peaked fluorescence spectrum [53], it has also been predicted by P.L. Knight [56] to split photo-electron energy peaks in resonant multi-photon ionization. It turns out that this coherence effect can also be transferred from one electron to another electron [57,58]. The coherence associated with resonant oscillations of a deeply bound inner electron can be transferred to the photoelectron spectrum of the loosely bound outer electron. This prediction was also confirmed experimentally by L. Di Mauro's group [59] in the two-photon ionization of calcium. In our case, the possibility of coherent oscillations of the captured electron is transferred to the *positron*. As the pair creation process is in principle a multi-particle process, it might be very worthwhile to examine this effect for those dynamical regimes, where more than just single electron is captured. In our present approach, the interaction between different electrons is only provided by the Pauli-exclusion principle, which means that the pair-creation process comes to a halt if all bound states of the binding potential are fully occupied [60]. This also means that the simultaneous capture of more than a single electron will have an interesting impact on the resonant Rabi-oscillations and therefore on the positron spectra. We will devote a future study to this intriguing question.

Acknowledgements Dandan Su would like to thank Dr. J. Zhang for his advice and acknowledges funding from the Institute of Physics of the Chinese Academy of Sciences for her Ph.D. research. This work has been supported by the NSF, Research Corporation, Strategic Priority Research Program of the Chinese Academy of Sciences (grant # XDA25010000 and XDB16010200) and National Natural Science Foundation of China (grant #11827807 and 11974419).

References

[1] For a comprehensive review, see A. Di Piazza, C. Müller, K.Z. Hatsagortsyan and C.H. Keitel, Rev. Mod. Phys. 84, 1177 (2012).

[2] B.S. Xie, Z.L. Li and S. Tang, Matter and Radiation at Extremes 2, 225 (2017).

[3] For a proposal for the development of the ELI program, see http://www.extreme-light-infrastructure.eu

[4] See the European x-ray laser project XFEL homepage at http://xfel.desy.de/

[5] The Vulcan petawatt project: http://www.clf.rl.ac.uk/Facilities/Vulcan/12248.aspx

[6] For work at the Chinese Academy of Sciences, see: http://highfield.iphy.ac.cn/

[7] For work at Shanghai Jiaotong University, see: http://ips.sjtu.edu.cn/

[8] C. Kohlfürst, M. Mitter, G. von Winckel, F. Hebenstreit and R. Alkofer, Phys. Rev. D 88, 045028 (2013).

[9] S.S. Dong, M. Chen, Q. Su and R. Grobe, Phys. Rev. A 96, 032120 (2017).

[10] F. Hebenstreit and F. Fillion-Gourdeau, Phys. Lett. B 739, 189 (2014).

[11] J. Unger, S.S. Dong, Q. Su and R. Grobe, Phys. Rev. A 100, 012518 (2019).

[12] M. Jiang, Q.Z. Lv, Z.M. Sheng, R. Grobe and Q. Su, Phys. Rev. A 87, 042503 (2013).

[13] F. Fillion-Gourdeau, E. Lorin and A.D. Bandrauk, Phys. Rev. Lett. 110, 013002 (2013).

[14] F. Fillion-Gourdeau, E. Lorin and A.D. Bandrauk, J. Phys. B 46, 175002 (2013).

[15] S. Tang, B.S. Xie, D. Lu, H.Y. Wang, L.B. Fu and J. Liu, Phys. Rev. A 88, 012106 (2013).

[16] Q. Wang, J. Liu and L.B. Fu, Sci. Rep. 6, 25292 (2016).

[17] L. Wang, B. Wu and B.S. Xie, Phys. Rev. A 100, 022127 (2019).

[18] V.B. Berestetskii, E.M. Lifshitz and L.P. Pitaevskii, "Quantum electrodynamics", Vol. 4 (Butterworth-Heinemann, 1982).

[19] D.D. Su, Y.T. Li, Q. Z. Lv and J. Zhang, Phys. Rev. D 101, 054501 (2020).

[20] M. Ruf, G.R. Mocken, C. Müller, K.Z. Hatsagortsyan and C.H. Keitel, Phys. Rev. Lett. 102, 080402 (2009).

[21] B. Thaller, “The Dirac equation” (Springer Verlag, Berlin, 1992).

[22] F. Sauter, Z. Phys. 69, 742 (1931); 73, 547 (1931).

[23] J.W. Braun, Q. Su and R. Grobe, Phys. Rev. A 59, 604 (1999).

[24] Q.Z. Lv and H. Bauke, Phys. Rev. D 96, 056017 (2017).

[25] Q.Z. Lv, Y. Liu, Y.J. Li, R. Grobe and Q. Su, Phys. Rev. Lett. 111, 183204 (2013).

[26] T. Cheng, Q. Su and R. Grobe, Contemp. Phys. 51, 315 (2010).

[27] D.M. Volkov, Z. Phys.94, 250 (1935).

[28] R.W. Brown and K.L. Kowalski, Phys. Rev. Lett. 51, 2355 (1983).

[29] D. Kidd, C. Covington, Y. Li and K. Varga, Phys. Rev. B 97, 024303 (2018).

[30] A. Di Piazza, Phys. Rev. Lett. 113, 040402 (2014).

[31] A. Di Piazza, Phys. Rev. A 91, 042118 (2015).

[32] D. Seipt, "Volkov States and Non-linear Compton Scattering in Short and Intense Laser Pulses" doi:10.3204/DESY-PROC-2016-04/Seipt [arXiv:1701.03692 [physics.plasm-ph]].

[33] L.S. Brown and T.W.B. Kibble, Phys. Rev. 133, 705 (1964).

[34] J.H. Eberly and A. Sleeper, Phys. Rev. 176, 1570 (1968).

[35] C. Harvey, T. Heinzl, A. Ilderton and M. Marklund, Phys. Rev. Lett. 109, 100402 (2012).

[36] C. Kohlfürst, H. Gies and R. Alkofer, Phys. Rev. Lett. 112, 050402 (2014).

[37] Q.Z. Lv, S. Dong, C. Lisowski, R. Pelphrey, Y.T. Li, Q. Su and R. Grobe, Phys. Rev. A 97, 053416 (2018).

[38] L.V. Keldysh, Zh. Eksp. Teor. Fiz. 47, 1945 (1964); Sov. Phys. JETP20, 1307 (1965).

[39] A.M. Perelomov, V.S. Popov and M.V. Terent'ev, Zh. Eksp. Teor. Fiz.50, 1393 (1966); Sov. Phys. JETP 23, 924 (1966).

[40] F.H.M. Faisal, J. Phys. B 6, L89 (1973).

[41] H.R. Reiss, Phys. Rev. A 22, 1786 (1980).

[42] H.R. Reiss, Prog. Quantum Electron.16, 1 (1992).

[43] W. Greiner, B. Müller and J. Rafelski, "Quantum Electrodynamics of Strong Fields" (Springer, Heidelberg, 1985).

[44] Y. Liu, M. Jiang, Q.Z. Lv, Y.T. Li, R. Grobe and Q. Su, Phys. Rev. A 89, 012127 (2014).

[45] Y. Liu, Q.Z. Lv, Y.T. Li, R. Grobe and Q. Su, Phys. Rev. A 91, 052123 (2015).

[46] N.B. Delone and V.P. Krainov, Phys.-Usp. 42, 669 (1999).

[47] F.H.M. Faisal, "Theory of multiphoton processes" (Springer Science & Business Media 1987).

[48] V. Vitanov, B.W. Shore, L. Yatsenko, K. Bohmer, T. Halfmann, T. Rickes, K. Bergmann, Opt. Commun. 199, 117 (2001).

[49] M. Jiang, W. Su, Z.Q. Lv, X. Lu, Y.J. Li, R. Grobe and Q. Su, Phys. Rev. A 85, 033408 (2012).

[50] M. Jiang, Z.Q. Lv, Z.M. Sheng, R. Grobe and Q. Su, Phys. Rev. A 87, 042503 (2013).

[51] L. Allen and J.H. Eberly, "Optical resonance and two-level atoms" (John Wiley & Sons, Inc., New York, 1975).

[52] S.H. Autler and C.H. Townes, Phys. Rev. 100, 703 (1955).

[53] B.R. Mollow, Phys. Rev. A 5, 2217 (1972).

[54] Limitations to the "node" model are discussed in B. King and H. Hu, Phys. Rev. D 94, 125010 (2016).

[55] Q.Z. Lv, S. Dong, Y.T. Li, Z.M. Sheng, Q. Su and R. Grobe, Phys. Rev. A 97, 022515 (2018).

[56] P.L. Knight, J. Phys. B 11, L511 (1978).

[57] R. Grobe and J.H. Eberly, Phys. Rev. A 48, 623 (1993).

[58] R. Grobe and S.L. Haan, J. Phys. B 27, L735 (1994).

[59] B. Walker, M. Kaluza, B. Sheehy, P. Agostini and L.F. DiMauro, Phys. Rev. Lett. 75, 633 (1995).

[60] P. Krekora, K. Cooley, Q. Su and R. Grobe, Phys. Rev. Lett. 95, 070403 (2005).